

# Theoretical Study of the $^{67}\text{Zn}$ Electric-Field-Gradient Tensors in Zinc(II) Coordination Complexes

Ramsey Ida and Gang Wu\*

Department of Chemistry, Queen's University, Kingston, Ontario, Canada K7L 3N6

Received: May 15, 2002; In Final Form: August 20, 2002

Electric-field-gradient (EFG) tensors at the zinc nuclear site were calculated using quantum mechanical methods for a series of zinc(II) coordination complexes. The accuracy of the calculated  $^{67}\text{Zn}$  EFG results at restricted Hartree–Fock (RHF) and density functional theory (DFT) levels was evaluated by comparing them with experimental solid-state  $^{67}\text{Zn}$  NMR data. Theoretical  $^{67}\text{Zn}$  EFG results at the B3LYP level using medium basis sets of 6-31G(f) for Zn and 6-31G(d) for ligand atoms were in good agreement with experimental  $^{67}\text{Zn}$  NMR data.

## 1. Introduction

Zinc is required as an integral constituent in a large number of enzymes.<sup>1,2</sup> To study the catalytic or structural role of zinc ions in these biological systems, it is desirable to have a technique that can probe the chemical environment at the zinc site. In the absence of X-ray crystallographic data, direct detection of the Zn(II) ions bound to a biological macromolecule is a difficult task because routine analytical techniques such as UV/vis, electron spin resonance (ESR), and solution NMR spectroscopy are not suitable for studying diamagnetic  $d^{10}$  Zn(II) ions. As a result, spectroscopic studies of metal binding sites in zinc-containing proteins have essentially relied on the utility of surrogate metal probes (e.g., Mn, Co, and Cd).<sup>3–5</sup>

Recently, solid-state  $^{67}\text{Zn}$  NMR spectroscopy has emerged as a viable method for detecting Zn(II) ions even in large molecular systems.<sup>6–14</sup> During these  $^{67}\text{Zn}$  NMR studies, it has become increasingly apparent that a better understanding of the  $^{67}\text{Zn}$  NMR properties is needed. One fundamental question is how the  $^{67}\text{Zn}$  NMR tensors, both the chemical shift tensor and the electric-field-gradient (EFG) tensor, are related to the chemical environment and molecular structure. One way to decipher this NMR property/structure relationship is to use quantum-mechanical calculations. To the best of our knowledge, quantum-mechanical  $^{67}\text{Zn}$  EFG calculations have been attempted only for simple ionic solids such as ZnO,<sup>15</sup> ZnAl<sub>2</sub>O<sub>4</sub>, and ZnFe<sub>2</sub>O<sub>4</sub>;<sup>16</sup> no theoretical study has been reported for the  $^{67}\text{Zn}$  EFG tensors in Zn(II) coordination complexes. The fact that a reasonable amount of reliable  $^{67}\text{Zn}$  EFG data has been accumulated in the past several years from experimental solid-state NMR studies makes the theoretical examination of  $^{67}\text{Zn}$  EFG tensors timely and possible. In this paper, we report a systematic quantum-mechanical investigation for the  $^{67}\text{Zn}$  EFG tensors in six Zn(II) coordination complexes: zinc acetate dihydrate (**1**), bis(acetato)bis(imidazole)zinc (**2**), tetrakis(imidazole)zinc perchlorate (**3**), tetrakis(thiourea)zinc nitrate (**4**), zinc formate dihydrate (**5**), and bis(acetato)bis(urea)zinc (**6**). These Zn(II) coordination complexes were chosen because both reliable X-ray crystallographic and solid-state  $^{67}\text{Zn}$  NMR data are available in the literature. Furthermore, single-crystal  $^{67}\text{Zn}$  NMR

studies have been reported for compounds **1** and **5** so that not only the magnitude but also the orientation of the  $^{67}\text{Zn}$  EFG tensor is known in the molecular frame of reference. This precise information is useful in determining the accuracy of the computed EFG results. The primary objective of the present study is to evaluate the applicability of current computational methods for calculating  $^{67}\text{Zn}$  EFG tensors in molecular complexes. In this study, we use a general molecular cluster approach to model the Zn(II) site in the crystal lattice. For Zn(II) coordination complexes examined in this study, the Zn(II) center is generally surrounded by ligand molecules such as imidazole and acetate groups. This is somewhat different from the ionic network solids such as ZnO and ZnAl<sub>2</sub>O<sub>4</sub>, for which it is important to take into consideration the lattice periodicity. For this reason, we usually include ligand molecules only from the first coordination sphere, with only one exception.

## 2. Computational Details

All molecular cluster models were constructed using experimental geometries obtained from X-ray diffraction experiments. In cases where hydrogen atom positions were not reported in the X-ray studies, standard bond lengths (C–H: 1.100 Å; N–H: 1.020 Å) were used to generate hydrogen atom positions. Detailed descriptions for each molecular cluster model will be given in the next section.

All EFG calculations were performed using the Gaussian 98 suite of programs<sup>17</sup> on a SunFire 6800 symmetric multiprocessor system (24 × 900-MHz processors and 24 GB of memory). Three all-electron basis sets were used for Zn: (1) fully optimized uncontracted basis set of Wachters,<sup>18</sup> (2) first-order polarized basis set of Kellö and Sadlej,<sup>19</sup> and (3) 6-31G(f) basis set of Rassolov et al.<sup>20</sup> The Wachters uncontracted basis set consists of 14s, 9p, and 4d Gaussian primitives. The basis set of Kellö and Sadlej (denoted as the KS basis set in this study) employs a contraction scheme of (16s12p6d4f) → [9s7p3d2f]. The 6-31G(f) basis set has a contraction scheme of (22s14p4d) → [5s4p2d] with a single set of f-type polarization functions (exponent 0.8). Standard basis sets of 6-31G(d) and 6-311++G-(3df,3pd) were used for ligand atoms. Calculations were carried out at both the restricted Hartree–Fock (RHF) level and the density functional theory (DFT) level. The B3LYP hybrid functional<sup>21</sup> was used in the DFT calculations. For a 37-atom

\* Corresponding author. E-mail: gangwu@chem.queensu.ca. Fax: +1-613-533-6669.

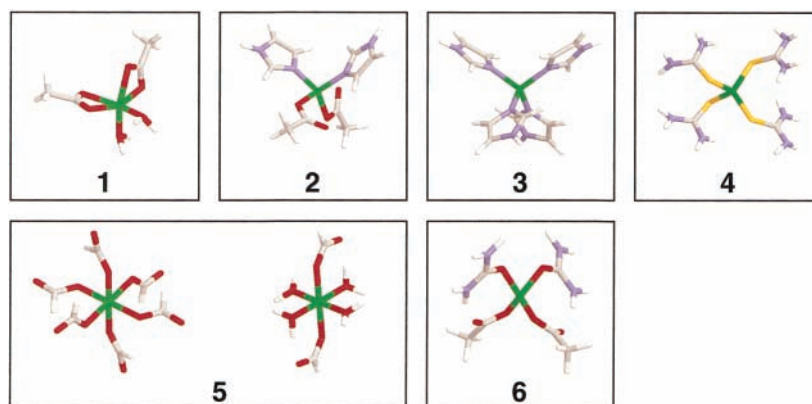


**Figure 1.** Molecular cluster models for compounds 1–6.

cluster (371 basis functions and 793 primitives), the CPU time of a typical B3LYP EFG calculation was approximately 26 min with 8 processors and 256 MB of memory. The largest cluster model attempted in this study contains 189 atoms (2244 basis functions and 4536 primitives). For this large cluster, 12 processors with 768 MB of memory were allocated, and the CPU time was 27 h at the B3LYP/6-31G(f)/6-31G(d) level.

In solid-state <sup>67</sup>Zn NMR experiments, the measurable quadrupole parameters are the nuclear quadrupole coupling constant ( $C_Q$ ) and the asymmetry parameter ( $\eta_Q$ ). These two parameters are related to the principal components of the corresponding EFG tensor ( $V_{XX}$ ,  $V_{YY}$ ,  $V_{ZZ}$ ) in the following fashion:

$$C_Q(\text{MHz}) = \frac{eQV_{ZZ}}{h} = -35.244 \times V_{ZZ}(\text{au}) \quad (1)$$

$$\eta_Q = \left| \frac{V_{XX} - V_{YY}}{V_{ZZ}} \right| \quad (2)$$

where where  $|V_{ZZ}| \geq |V_{YY}| \geq |V_{XX}|$  and  $V_{ZZ} + V_{YY} + V_{XX} = 0$ . The coefficient in eq 1 is obtained using the <sup>67</sup>Zn quadrupole moment value recommended by Pyykkö,<sup>22</sup>  $Q(^{67}\text{Zn}) = 15.0 \times 10^{-30} \text{ m}^2$ . The computed EFG tensor components are reported in atomic units ( $1 \text{ au} = 9.717365 \times 10^{21} \text{ V m}^{-2}$ ). In this study, experimental quadrupole parameters ( $C_Q$  and  $\eta_Q$ ) are converted to EFG tensor components for comparison. However, because the sign of  $V_{ZZ}$  is not available in solid-state <sup>67</sup>Zn NMR studies, we assume the same sign for the observed and calculated  $V_{ZZ}$  components.

### 3. Results and Discussion

The molecular cluster models used for the <sup>67</sup>Zn EFG calculations are shown in Figure 1. In each of these models, only ligands from the first coordination sphere around the Zn(II) ion were considered at this stage (vide infra). Because the crystal structure of  $\text{Zn}(\text{acetate})_2 \cdot 2\text{H}_2\text{O}$  (**1**) reported in an early X-ray diffraction study<sup>23</sup> was inaccurate, the most recent X-ray report for this compound was used.<sup>24</sup> Unfortunately, the authors of this recent study also made a mistake regarding the geometry of the water molecules of hydration. In particular, the H–O–H angle was assumed *incorrectly* to be 120°. Furthermore, the orientation of the water molecules in the crystal lattice is somewhat unusual in that one of the O–H···O hydrogen bond angles is 121°, clearly far from the usually preferred linear arrangement. For these reasons, we decided to perform a geometry optimization to determine the precise geometry and orientation of the two water molecules of hydration in compound **1**. The molecular model for partial geometry optimization

consists of all of the first coordination sphere ligands as shown in Figure 1 and four neighboring acetate groups (not shown) that serve as hydrogen bond acceptors.<sup>24</sup> After partial geometry optimization at the B3LYP/6-31G(f)/6-31G(d) level, both the geometry and the orientation of the water molecules are reasonable (O–H: 1.010, 1.022 Å;  $\angle\text{H–O–H}$ : 105.47°;  $\angle\text{O–H}\cdots\text{O}$ : 173.2°, 175.8°). This model was used in the <sup>67</sup>Zn EFG calculations for compound **1**. As seen from Figure 1, the Zn(II) ion in **1** is coordinated by two bidentate acetate ligands and two water molecules in a very distorted octahedral fashion. The Zn–O<sub>w</sub> distance, 1.987 Å, is significantly shorter than the two Zn–O<sub>acetate</sub> bonds, 2.179 and 2.189 Å. The Zn(II) ion is located on the crystallographic 2-fold axis, which bisects the O<sub>w</sub>–Zn–O<sub>w</sub> angle.

The Zn(II) ion in bis(acetato)bis(imidazole)zinc (**2**) is tetrahedrally coordinated by two imidazole molecules and two acetate ligands.<sup>25</sup> The two independent Zn–N bond distances are very similar, 1.996 and 2.003 Å, whereas the two Zn–O distances are somewhat different, 1.965 and 1.991 Å. Each imidazole molecule is hydrogen bonded to an acetate group from the neighboring molecule. The Zn(II) ion in  $[\text{Zn}(\text{imidazole})_4](\text{ClO}_4)_2$  (**3**) is coordinated by four imidazole ligands.<sup>26</sup> The Zn(II) ion also lies on a crystallographic 2-fold axis. The two Zn–N distances, 1.997 and 2.001 Å, are essentially identical to those found in **2**. The N–Zn–N angles are all within 4.1° of a perfect tetrahedral geometry. The imidazole molecules in **3** are involved in hydrogen bonding to the anions. The hydrogen bond distances are 2.95 and 3.06 Å between the imidazole “pyrrole” N and the perchlorate O atoms. Because the perchlorate anions are quite far from the Zn(II) center (6.27–7.61 Å), they were not included in the cluster model. Similarly, the Zn(II) ion in  $[\text{Zn}(\text{thiourea})_4](\text{NO}_3)_2$  (**4**) is also in a tetrahedral environment, coordinating to four thiourea molecules.<sup>27</sup> The S–Zn–S angles are between 100.0 and 120.5°, suggesting a larger deviation from a perfect tetrahedral geometry than for the Zn(II) ion in compound **3**. The Zn–S bonds, 2.324 and 2.361 Å, are much longer than all of the Zn–O bonds mentioned above. The thiourea molecules are hydrogen bonded to the nitrate groups. Again, because the nitrate groups are far from the Zn(II) center (5.71–7.67 Å), they were not included in the model shown in Figure 1. Compound **5**,  $\text{Zn}(\text{formate})_2 \cdot 2\text{H}_2\text{O}$ , crystallizes in a monoclinic form with space group  $P2_1/c$ .<sup>13,28</sup> There are two crystallographically distinct Zn sites in the asymmetric unit. One Zn site is coordinated by six formate groups, and the other, by four water molecules and two formate groups. The Zn–O distances are very similar at both Zn sites, 2.052–2.166 Å. Both sites have a slightly distorted octahedral arrangement. Finally, the Zn(II) ion in bis(acetato)bis(urea)Zn (**6**) is also four-

**TABLE 1: Experimental Solid-State  $^{67}\text{Zn}$  NMR Data for the Zinc(II) Complexes Examined in This Study**

compound	Zn coordination	$\delta_{\text{iso}}$ (ppm)	$C_Q$ (MHz)	$\eta_Q$	ref
(1) Zn(acetate) $_2$ ·2H $_2$ O	ZnO $_6$	0	5.20 $\pm$ 0.03	0.898 $\pm$ 0.017	9
(2) Zn(imidazole) $_2$ (acetate) $_2$	ZnN $_2$ O $_2$	155	8.2 $\pm$ 0.2	0.6 $\pm$ 0.1	10
(3) Zn(imidazole) $_4$ (ClO $_4$ ) $_2$	ZnN $_4$	291	2.80 $\pm$ 0.05	0.4 $\pm$ 0.1	8
(4) Zn(thiourea) $_4$ (NO $_3$ ) $_2$	ZnS $_4$	350	3.15 $\pm$ 0.05	1.00 $\pm$ 0.05	8
(5) Zn(formate) $_2$ ·2H $_2$ O	site 1 ZnO $_6$	-24	6.34 $\pm$ 0.05	0.98 $\pm$ 0.01	13
	site 2 ZnO $_6$	-26	9.63 $\pm$ 0.06	0.45 $\pm$ 0.02	13
(6) Zn(urea) $_2$ (acetate) $_2$	ZnO $_4$	200	12.85 $\pm$ 0.05	0.85 $\pm$ 0.05	30

**TABLE 2: Calculated  $^{67}\text{Zn}$  EFG Tensor Components Using the 6-31G(d) Basis Set for Ligand Atoms<sup>a,b</sup>**

compound	Zn basis set	RHF			B3LYP		
		$V_{ZZ}$	$V_{YY}$	$V_{XX}$	$V_{ZZ}$	$V_{YY}$	$V_{XX}$
<b>1</b>	Wachters	-0.0605	0.0483	0.0373	0.0518	-0.0416	-0.0102
	KS	-0.0768	0.0395	0.0373	-0.1263	0.1026	0.0236
	6-31G(f)	-0.0836	0.0456	0.0380	-0.1308	0.0909	0.0399
	exptl				-0.1475	0.1400	0.0075
<b>2</b>	Wachters	-0.3774	0.2100	0.1674	-0.2916	0.1773	0.1143
	KS	-0.3033	0.1904	0.1128	-0.2310	0.1786	0.0524
	6-31G(f)	-0.2127	0.1551	0.0576	-0.1910	0.1757	0.0153
	exptl				-0.2327	0.1884	0.0442
<b>3</b>	Wachters	-0.1491	0.0856	0.0635	-0.1164	0.0618	0.0546
	KS	-0.1231	0.0644	0.0587	-0.0927	0.0565	0.0362
	6-31G(f)	-0.1056	0.0703	0.0353	-0.0911	0.0848	0.0063
	exptl				-0.0794	0.0556	0.0238
<b>4</b>	Wachters	0.0776	-0.0429	-0.0347	0.0367	-0.0335	-0.0032
	KS	-0.0304	0.0295	0.0009	-0.0392	0.0328	0.0064
	6-31G(f)	-0.0362	0.0350	0.0011	-0.1291	0.0807	0.0484
	exptl				-0.0894	0.0894	0.0000
<b>5 (site 1)</b>	Wachters	-0.2593	0.2437	0.0156	-0.2111	0.2007	0.0105
	KS	-0.2326	0.2240	0.0085	-0.1855	0.1763	0.0091
	6-31G(f)	-0.1838	0.1724	0.0114	-0.1568	0.1383	0.0184
	exptl				-0.1799	0.1781	0.0018
<b>5 (site 2)</b>	Wachters	-0.0828	0.0563	0.0265	-0.0843	0.0689	0.0154
	KS	-0.1287	0.1316	-0.0029	-0.1523	0.1618	-0.0095
	6-31G(f)	<u>-0.0992</u>	<u>0.1096</u>	-0.0104	<u>-0.1464</u>	<u>0.1494</u>	-0.0030
	exptl				-0.2732	0.1981	0.0751
<b>6</b>	Wachters	-0.7552	0.6725	0.0827	-0.6087	0.5320	0.0767
	KS	-0.6449	0.6206	0.0243	-0.4951	0.4876	0.0075
	6-31G(f)	-0.4422	0.4211	0.0211	-0.3407	0.3328	0.0079
	exptl				-0.3646	0.3374	0.0272

<sup>a</sup> EFG tensor components  $V_{XX}$ ,  $V_{YY}$ , and  $V_{ZZ}$  are reported in atomic units (1 au =  $9.717365 \times 10^{21}$  V m $^{-2}$ ). <sup>b</sup> Underlined data represent situations where a switch between  $V_{ZZ}$  and  $V_{YY}$  components occurs because of the fact that these two components are essentially the same. See text for discussions.

coordinate.<sup>29</sup> Although the four Zn–O distances are similar, 1.970–1.997 Å, the O–Zn–O angles deviate significantly from a perfect tetrahedral geometry, 89.5–126.8°. Therefore, a large  $C_Q$  value is expected for the Zn site in compound **6**.

Experimental solid-state  $^{67}\text{Zn}$  NMR data for compounds **1–6** are summarized in Table 1. Compounds **1–6** constitute a good test set for the following reasons. First, these Zn(II) coordination complexes have recently been studied by solid-state  $^{67}\text{Zn}$  NMR and, in two cases, by single-crystal  $^{67}\text{Zn}$  NMR. Second, these complexes exhibit very different  $C_Q(^{67}\text{Zn})$  values (over a range of ca. 10 MHz). Third, they represent a variety of coordination environments, including both tetrahedral and octahedral coordination arrangements and containing common ligand atoms such as O, N, and S. Fourth, reliable single-crystal X-ray diffraction data are available for these Zn complexes.

Table 2 shows the computed  $^{67}\text{Zn}$  EFG tensors for compounds **1–6**. Comparisons between the calculated and observed results at various levels of theory are shown in Figure 2. For a given basis set, the calculations at the B3LYP level show consistently better agreement with the experimental data than the corre-

sponding calculations at the RHF level. It is also apparent that the uncontracted basis set of Wachters for Zn cannot generate useful  $^{67}\text{Zn}$  EFG data. The KS basis set (16s12p6d4f/9s7p3d2f) is perhaps the minimal basis set for  $^{67}\text{Zn}$  EFG calculations. Although the 6-31G(f) basis set (22s14p4d1f/5s4p2d1f) is similar in size to the KS basis set, improvement of 6-31G(f) over KS is noticeable from the calculated results. This may be attributed to the fact that 6-31G(f) is a fully optimized basis set because both the contraction coefficients and the exponents were simultaneously optimized.<sup>20</sup> In contrast, the KS basis set is not fully optimized. As seen from Figure 2, the best calculated results for the  $^{67}\text{Zn}$  EFG tensor components exhibit a standard error of 0.03 au (1 au corresponds to 35.244 MHz for  $^{67}\text{Zn}$ ). Because the signs of the EFG tensor components were not available from solid-state NMR experiments, we assumed that the experimental EFG tensor components have the same signs as those calculated at the B3LYP/6-31G(f) level. The fact that the calculations at the RHF and B3LYP levels show similar results may indicate that electron correlation is not important in the present Zn systems. This is consistent with the theoretical

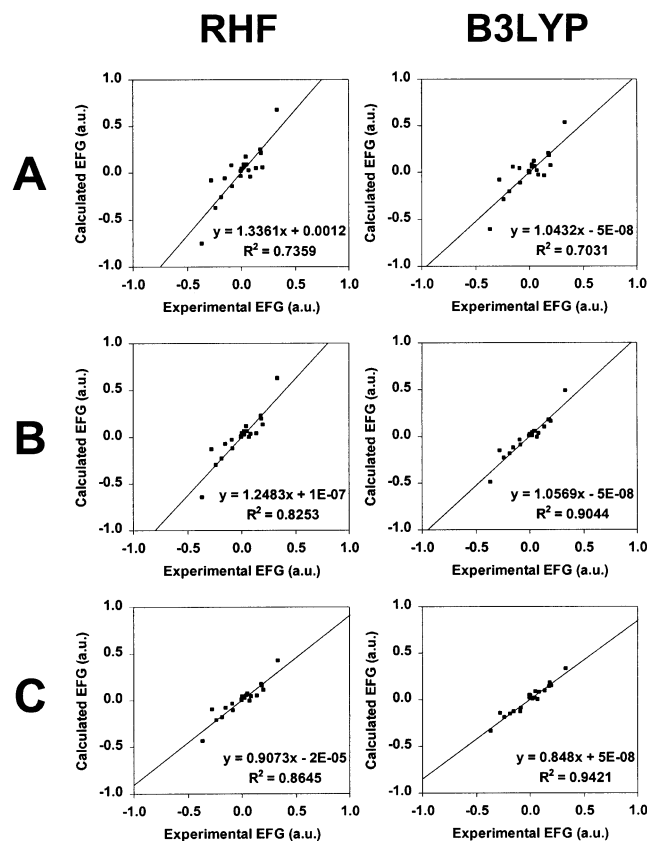


**Figure 2.** Comparison between experimental and calculated <sup>67</sup>Zn EFG tensor components for compounds 1–6. The basis sets used for Zn are (A) Wachters, (B) KS, and (C) 6-31G(f).

**TABLE 3: Calculated <sup>67</sup>Zn EFG Tensor Components at the B3LYP/6-31G(f)/6-311++G(3df,3pd) Level <sup>a,b</sup>**

compound	$V_{ZZ}$	$V_{YY}$	$V_{XX}$
1	-0.0851	0.0671	0.0180
2	-0.1746	0.1219	0.0526
3	-0.0866	0.0658	0.0208
4	-0.0716	0.0714	0.0002
5 (site 1)	-0.1685	0.1602	0.0083
5 (site 2)	-0.1173	0.1190	-0.0017
6	-0.3977	0.3695	0.0282

<sup>a</sup> EFG tensor components  $V_{XX}$ ,  $V_{YY}$ , and  $V_{ZZ}$  are reported in atomic units (1 au =  $9.717365 \times 10^{21}$  V m<sup>-2</sup>). <sup>b</sup> Underlined data represent situations where a switch between  $V_{ZZ}$  and  $V_{YY}$  components occurs because of the fact that these two components are essentially the same. See text for discussion.

EFG results of Hemmingsen and Ryde for cadmium(II) complexes.<sup>31</sup> Because both correlation and relativistic effects are expected to be small for Zn(II) coordination complexes, it may not be surprising that our nonrelativistic calculations have produced reasonably good <sup>67</sup>Zn EFG results.

To evaluate the dependence of the <sup>67</sup>Zn EFG tensors on the basis set used for ligand atoms, we also performed B3LYP calculations using 6-31G(f) for Zn and a larger basis set, 6-311++G(3df,3pd), for ligand atoms. The computed EFG results are presented in Table 3. In general, the quality of the calculated EFG results at the 6-311++G(3df,3pd) level (slope = 0.840,  $R^2 = 0.9079$ ) is similar to that computed at the 6-31G(d) level (slope = 0.848,  $R^2 = 0.9421$ ). This suggests that the quality of the computed <sup>67</sup>Zn EFG data is determined primarily by the quality of the basis set used for the Zn atom.

Careful examination of the data presented in Tables 2 and 3 indicates that the tensor components for the hydrated Zn site

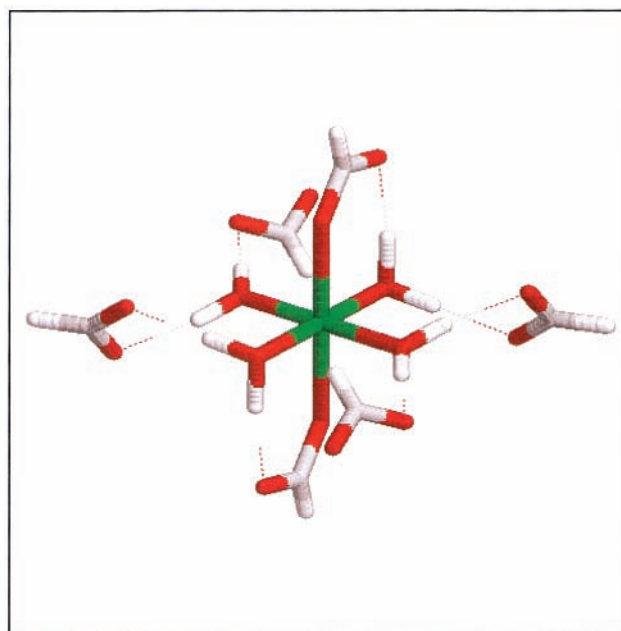


**Figure 3.** Molecular cluster model containing four additional formate groups from the second coordination sphere for site 2 of compound 5. Hydrogen bonds are indicated by the dashed lines.

of zinc formate dihydrate (site 2 of 5) exhibit an unusually large deviation from the experimental data. Furthermore, as indicated in Tables 2 and 3, the calculations using the KS and 6-31G(f) basis sets yielded positive  $V_{ZZ}$  components for site 2 of 5, which is opposite to the sign of  $V_{ZZ}$  for other sites. The unique structural feature of this Zn site is the presence of four water molecules in the first coordination sphere. More importantly, these water molecules are involved in strong hydrogen bonding to the neighboring formate groups. The large discrepancy observed between the experimental and calculated results may suggest that the ligands from the second coordination sphere are also important in this case. In addition to the strong H-bonding interactions, water molecules are much smaller in size than other ligand molecules such as acetate and imidazole groups. Consequently, ligands from the second coordination sphere are also quite close to the Zn center for site 2 of 5, making it possible to have an electrostatic effect from nearby ligands. To further evaluate the influence of hydrogen-bonded ligands from the second coordination sphere, we constructed a larger molecular cluster model for site 2 of 5, which includes four additional formate groups, as shown in Figure 3. For this new model, the calculated <sup>67</sup>Zn EFG results at the B3LYP/6-31G(f)/6-31G(d) level are  $V_{ZZ} = -0.2029$ ,  $V_{YY} = 0.1428$ , and  $V_{XX} = 0.060$ . Indeed these results are in better agreement with the experimental data ( $V_{ZZ} = -0.2732$ ,  $V_{YY} = 0.1981$ , and  $V_{XX} = 0.0751$ ) than the results presented in Tables 2 and 3. In addition, the sign for  $V_{ZZ}$  is now negative, consistent with that for other Zn(II) sites. As seen from Figure 4, when these new data are used for site 2 of 5, a much better correlation is observed between the calculated and experimental data (slope = 0.880 and  $R^2 = 0.9685$ ). Further examination of the calculated results reveals the reason for such a sign reversal. As seen from Tables 2 and 3, the calculated EFG tensors have close to axial symmetry for site 2 of 5. Therefore, a small variation in the magnitude of  $V_{ZZ}$  and  $V_{YY}$  would result in a switch of the two components, leading to a sign reversal of  $V_{ZZ}$ . For this reason, the observed sign reversal mentioned above is not as drastic a change as it may appear to be at first sight. The negative sign of  $V_{ZZ}$  in this particular situation is further confirmed by considering an even

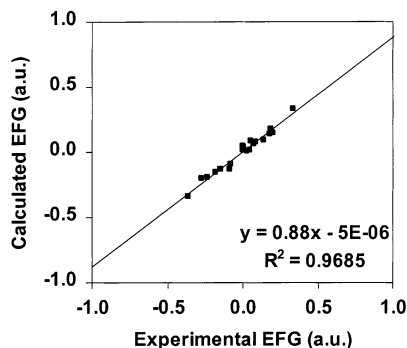


**Figure 4.** Comparison between experimental and calculated  $^{67}\text{Zn}$  EFG tensor components using the cluster models shown in Figures 1 and 3. The calculations are at the B3LYP/6-31G(f)/6-31G(d) level.

larger cluster to model the crystal lattice around the Zn(II) site (site 2 of **5**). This cluster contains 9 Zn atoms, 12 water molecules, and 36 formate groups (a total of 189 atoms) where the target Zn atom is at the center of the cluster. We also found that it is important to maintain the symmetry of the cluster so that long-range electrostatic effects can be minimized.

**EFG Tensor Orientations.** It is clear from the above discussion that quantum-mechanical calculations at the B3LYP/6-31G(f) level can reproduce the experimental EFG tensor components within a reasonable degree of accuracy. To make a full assessment of the accuracy of any second-rank tensor, it is important to evaluate not only the magnitude of the tensor components but also their orientations in the molecular frame. In this regard, two recent single-crystal  $^{67}\text{Zn}$  NMR studies<sup>9,13</sup> make it possible for us to examine further the calculated  $^{67}\text{Zn}$  EFG tensor orientations for compounds **1** and **5**.

Figure 5 shows the calculated orientations of the  $^{67}\text{Zn}$  EFG tensors for compounds **1** and **5**. For compound **1**,  $V_{ZZ}$  is found to lie in the crystallographic  $ac$  plane. The angle between  $V_{ZZ}$  and the shorter Zn–O<sub>acetate</sub> bond (2.179 Å) is 58.4°. This is approximately 33° off the direction of  $V_{ZZ}$  as reported by Vosegaard et al.<sup>9</sup> We found that  $V_{XX}$  is along the crystallographic  $b$  axis. This is also the direction that bisects the O<sub>W</sub>–Zn–O<sub>W</sub> angle as well as the crystallographic 2-fold axis as mentioned earlier. Vosegaard et al.<sup>9</sup> also reported that  $V_{XX}$  is along this direction. However, these authors usually use a slightly different definition for EFG tensor components. That is, their  $V_{XX}$  component corresponds to our  $V_{YY}$ . Therefore, there exists an apparent discrepancy between the tensor orientation shown in Figure 5 and that reported by Vosegaard et al.<sup>9</sup> The reason for this discrepancy is unclear at this time.

For the anhydrous Zn site in zinc formate dihydrate (site 1 of **5**), we found that  $V_{ZZ}$  is 8.1° off the longest Zn–O<sub>formyl</sub> bond (2.150 Å) and that  $V_{YY}$  is 5.8° off the shortest Zn–O<sub>formyl</sub> bond (2.071 Å). At first glance, the above tensor orientation is very different from that reported by Lipton et al.<sup>13</sup> from a single-crystal  $^{67}\text{Zn}$  NMR study. However, because the EFG tensor at this Zn site is essentially axially symmetric ( $\eta_Q = 0.98 \pm 0.01$ ), there is little difference between  $V_{ZZ}$  and  $V_{YY}$ , i.e.,  $|V_{ZZ}| \sim |V_{YY}|$ . It should also be noted that the so-called “second largest tensor element” in the study of Lipton et al.<sup>13</sup> corresponds to the  $V_{YY}$  component in this study. After considering these factors, we find that our EFG tensor orientation is indeed in excellent agreement with the single-crystal NMR result. For the hydrated Zn site in zinc formate dihydrate (site 2 of **5**), we found that  $V_{ZZ}$  is 11.2° off the Zn–O<sub>formyl</sub> bond. Both  $V_{XX}$  and  $V_{YY}$  are located approximately in the plane formed by four water molecules with the  $V_{YY}$  component making an angle of 18.7° with respect to the shortest Zn–O<sub>W</sub> bond (2.052 Å). In

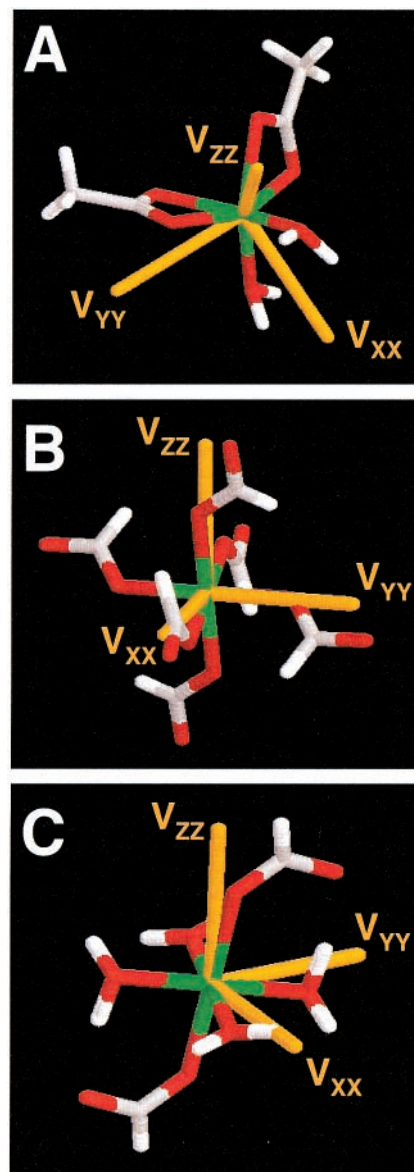


**Figure 5.** Orientations of the calculated  $^{67}\text{Zn}$  EFG tensors in (A) compound **1** and (B, C) compound **5**. The calculations are at the B3LYP/6-31G(f)/6-31G(d) level.

comparison, Lipton et al.<sup>13</sup> observed that the second largest component ( $V_{YY}$  in our notation) is 30° from the shortest Zn–O<sub>W</sub> bond. Therefore, the calculated  $^{67}\text{Zn}$  EFG tensor orientations are in agreement with the single-crystal NMR data for compound **5**.

#### 4. Conclusions

We have presented a theoretical examination of the  $^{67}\text{Zn}$  EFG tensors in several zinc(II) coordination complexes. We have been able to evaluate the accuracy of the current computational methods by comparing our calculated results with experimental solid-state NMR data. This work demonstrates that quantum-mechanical calculations at the B3LYP level with medium-size basis sets, 6-31G(f) for Zn and 6-31G(d) for other atoms, can yield reliable  $^{67}\text{Zn}$  EFG tensors for Zn(II) coordination complexes. The present work represents the first attempt to investigate the  $^{67}\text{Zn}$  EFG tensors in Zn(II) coordination complexes systematically by quantum-mechanical computations. We have discovered that it is often sufficient to consider only ligands from the first coordination sphere around the zinc atom. The

only exception to this general statement is that, if the Zn center of interest is bound to water molecules and the water molecules are involved in extensive H-bonding, ligands from the second coordination sphere must be included in the cluster model. This finding is important because water molecules often participate in Zn(II) ion binding in zinc-containing proteins. The implication of the present study is that it is possible to predict  $^{67}\text{Zn}$  EFG tensors for the Zn(II) sites in proteins. Although we have focused on EFG tensors, it should also be possible to examine the  $^{67}\text{Zn}$  magnetic (or chemical) shielding tensors using quantum-mechanical computations. Very little is known in this latter area; however, it is hoped that the present study will encourage further quantum-mechanical studies of these fundamental  $^{67}\text{Zn}$  NMR tensors.

**Acknowledgment.** We thank the Natural Sciences and Engineering Research Council (NSERC) of Canada for research and equipment grants. G.W. also thanks Queen's University for a Chancellor's Research Award (2000–2004) and the Ontario Government for a Premier's Research Excellence Award (2000–2004). All quantum-mechanical computations were performed at the High Performance Computing Virtual Laboratory (HPCVL) at Queen's University. We are grateful to Hartmut Schmider for technical assistance in quantum-mechanical computations and to Alan Wong for assistance in preparing several figures.

## References and Notes

- (1) Lippard, S. J.; Berg, J. M. *Principles of Bioinorganic Chemistry*; University Science Books: Mill Valley, CA, 1994.
- (2) Frausto da Silva, J. J. R.; Williams, R. J. P. *The Biological Chemistry of the Elements*; Oxford University Press: Oxford, U.K., 1991.
- (3) Summers, M. F. *Coord. Chem. Rev.* **1988**, *86*, 43.
- (4) McAteer, K.; Lipton, A. S.; Ellis, P. D. *Encyclopedia of Nuclear Magnetic Resonance*; Grant, D. M., Harris, R. K., Eds.; Wiley: Chichester, U.K., 1996; pp 1085–1091.
- (5) Öz, G.; Pountney, D. L.; Armitage, I. M. *Biochem. Cell Biol.* **1998**, *76*, 223.
- (6) Wu, G. *Biochem. Cell Biol.* **1998**, *76*, 429.
- (7) Wu, G. *Chem. Phys. Lett.* **1998**, *298*, 375.
- (8) Sham, S.; Wu, G. *Can. J. Chem.* **1999**, *77*, 1782.
- (9) Vosegaard, T.; Andersen, U.; Jakobsen, H. J. *J. Am. Chem. Soc.* **1999**, *121*, 1970.
- (10) Larsen, F. H.; Lipton, A. S.; Jakobsen, H. J.; Nielsen, N. C.; Ellis, P. D. *J. Am. Chem. Soc.* **1999**, *121*, 3783.
- (11) Lipton, A. S.; Buchko, G. W.; Sears, J. A.; Kennedy, M. A.; Ellis, P. D. *J. Am. Chem. Soc.* **2001**, *123*, 992.
- (12) Lipton, A. S.; Sears, J. A.; Ellis, P. D. *J. Magn. Reson.* **2001**, *151*, 48.
- (13) Lipton, A. S.; Smith, M. D.; Adams, R. D.; Ellis, P. D. *J. Am. Chem. Soc.* **2002**, *124*, 410.
- (14) Power, W. P.; Gu, J. Unpublished results.
- (15) Mitchell, D. W.; Sulaiman, S. B.; Sahoo, N.; Das, T. P.; Potzel, W.; Kalvius, G. M. *Phys. Rev. B* **1991**, *44*, 6728.
- (16) Mitchell, D. W.; Das, T. P.; Potzel, W.; Schiessl, W.; Karzel, H.; Steiner, M.; Köfferlein, M.; Hiller, U.; Kalvius, G. M.; Martin, A.; Schäfer, W.; Will, G.; Halevy, I.; Gal, J. *Phys. Rev. B* **1996**, *53*, 7684.
- (17) Frisch, M. J.; Trucks, G. W.; Schlegel, H. B.; Scuseria, G. E.; Robb, M. A.; Cheeseman, J. R.; Zakrzewski, V. G.; Montgomery, J. A., Jr.; Stratmann, R. E.; Burant, J. C.; Dapprich, S.; Millam, J. M.; Daniels, A. D.; Kudin, K. N.; Strain, M. C.; Farkas, O.; Tomasi, J.; Barone, V.; Cossi, M.; Cammi, R.; Mennucci, B.; Pomelli, C.; Adamo, C.; Clifford, S.; Ochterski, J.; Petersson, G. A.; Ayala, P. Y.; Cui, Q.; Morokuma, K.; Malick, D. K.; Rabuck, A. D.; Raghavachari, K.; Foresman, J. B.; Cioslowski, J.; Ortiz, J. V.; Stefanov, B. B.; Liu, G.; Liashenko, A.; Piskorz, P.; Komaromi, I.; Gomperts, R.; Martin, R. L.; Fox, D. J.; Keith, T.; Al-Laham, M. A.; Peng, C. Y.; Nanayakkara, A.; Gonzalez, C.; Challacombe, M.; Gill, P. M. W.; Johnson, B. G.; Chen, W.; Wong, M. W.; Andres, J. L.; Head-Gordon, M.; Replogle, E. S.; Pople, J. A. *Gaussian 98*, revision A.9; Gaussian, Inc.: Pittsburgh, PA, 1998.
- (18) Wachters, A. J. H. *J. Chem. Phys.* **1970**, *52*, 1033.
- (19) Kellö, V.; Sadlej, A. J. *Theor. Chim. Acta* **1995**, *91*, 353.
- (20) Rassolov, V. A.; Pople, J. A.; Ratner, M. A.; Windus, T. L. *J. Chem. Phys.* **1998**, *109*, 1223.
- (21) Becke, A. D. *J. Chem. Phys.* **1993**, *98*, 5648.
- (22) Pyykkö, P. *Mol. Phys.* **2001**, *99*, 1617.
- (23) van Niekerk, J. N.; Schoening, F. R. L.; Talbot, J. H. *Acta Crystallogr.* **1953**, *6*, 720.
- (24) Ishioka, T.; Murata, A.; Kitagawa, Y.; Nakamura, K. T. *Acta Crystallogr., Sect. C* **1997**, *53*, 1029.
- (25) (a) Chen, X.-M.; Xu, Z.-T.; Huang, X.-C. *J. Chem. Soc., Dalton Trans.* **1994**, 2331. (b) Chen, X.-M.; Ye, B.-H.; Huang, X.-C.; Xu, Z.-T. *J. Chem. Soc., Dalton Trans.* **1996**, 3465.
- (26) Bear, C. A.; Duggan, K. A.; Freeman, H. C. *Acta Crystallogr., Sect. B* **1975**, *31*, 2713.
- (27) Vega, E.; López-Castro, A.; Márquez, R. *Acta Crystallogr., Sect. B* **1978**, *34*, 2297.
- (28) Burger, N.; Fuess, H. Z. *Kristallogr.* **1977**, *145*, 346.
- (29) Yar, O.; Lessinger, L. *Acta Crystallogr., Sect. C* **1995**, *51*, 2282.
- (30) Wu, G. Unpublished results.
- (31) Hemmingsen, L.; Ryde, U. *J. Phys. Chem.* **1996**, *100*, 4803.